NASA TN D-799

TECHNICAL NOTE

D-799

INVESTIGATION OF THREE ANALYTICAL HYPOTHESES FOR DETERMINING MATERIAL CREEP BEHAVIOR UNDER VARIED LOADS, WITH AN APPLICATION TO 2024-T3 ALUMINUM-ALLOY SHEET IN TENSION AT 400° F

By Avraham Berkovits

Langley Research Center
Langley Field, Va.

NATIONAL AERONAUTICS AND SPACE ADMINISTRATION
WASHINGTON

May 1961

NATIONAL AERONAUTICS AND SPACE ADMINISTRATION

TECHNICAL NOTE D-799

INVESTIGATION OF THREE ANALYTICAL HYPOTHESES FOR DETERMINING MATERIAL CREEP BEHAVIOR UNDER VARIED LOADS, WITH AN APPLICATION TO 2024-T3 ALUMINUM-ALLOY SHEET IN TENSION AT 400° F *

By Avraham Berkovits

SUMMARY

Three existing hypotheses are formulated mathematically to estimate tensile creep strain under varied loads and constant temperature from creep data obtained under constant load and constant temperature. The hypotheses investigated include the time-hardening, strain-hardening, and life-fraction rules. Predicted creep behavior is compared with data obtained from tensile creep tests of 2024-T3 aluminum-alloy sheet at 400° F under cyclic-load conditions. A simplified method of calculating creep strain under varied loads is presented on the basis of an equivalent stress, derived from the life-fraction rule, which reduces the varied-load case to a constant-load problem. Creep strain in the region of interest for structural design and rupture times, determined from the hypotheses investigated, are in fair agreement with data in most cases, although calculated values of creep strain are generally greater than the experimental values because creep recovery is neglected in the calculations.

INTRODUCTION

Structural components of modern aircraft may be required to operate at elevated temperatures under varying or cyclic-load conditions for

*This paper is based in part upon a thesis entitled "Tensile Creep of 2024-T3 Aluminum-Alloy Sheet Under Varying Load Conditions" submitted by the author in partial fulfillment of the requirements for the degree of Master of Science in Engineering Mechanics, Virginia Polytechnic Institute, Blacksburg, Virginia, March 1960.

sufficient time to cause significant creep in the structure. For this reason recent interest has developed in problems of creep under varying load and varying temperature. Several methods are available for predicting creep strain and rupture under varying loads and temperatures (refs. 1 and 2); however, relatively few results are available which compare the theoretical studies with experimental information. In the correlations which have been published, the analyses have most frequently been concerned with large values of strain that are generally beyond the range of usual interest for aircraft structures. The range of creep strains which appear to be of most practical importance in aircraft structural applications involves small creep strains of the order of 0.005 or less. (See, for example, refs. 3 and 4.)

The present paper presents an attempt to estimate creep strain under very low frequency cyclic loads and constant temperature, from creep data obtained under constant load and constant temperature. The time-hardening, strain-hardening, and life-fraction hypotheses (ref. 5) are expressed mathematically so that creep strain under cyclic loads may be calculated from creep data obtained at constant load. Results obtained from these hypotheses are compared with one another and with data obtained experimentally. Tensile creep test results were obtained from 2024-T3 aluminum-alloy sheet at 400° F.

SYMBOLS

A, C, k, σ_o	empirical creep constants
E	Young's modulus, ksi
N	number of load cycles to cause failure
t	time, hr
ϵ	total strain
σ	stress, ksi
σ_e	equivalent stress, ksi
σ_{ty}	tensile yield stress, ksi

Subscripts:

A,B,C	designation of points in figure 1

i,j,m,n integers

r rupture

MATHEMATICAL FORMULATION OF CREEP HYPOTHESES

Many equations are available in the literature describing material creep behavior under constant load and constant temperature. Such relations are generally not applicable to the entire creep curve. In cases involving long-time creep at low stresses, secondary creep may be considered most important, whereas in other cases primary creep may be of most significance. It has been shown (refs. 3 and 4) that creep strain between 0.002 and 0.005 represents the maximum creep strain of interest for most aircraft structural applications. Thus consideration of primary creep will generally be sufficient, and the emphasis throughout the analytical formulation of the creep problem in the present study will be on the primary creep region.

Creep Relation for Constant Load and Constant Temperature

The calculation of primary creep strain under varied loads, as presented in this investigation, is based on a knowledge of the material creep behavior under constant load. In this study the creep relation for total strain of the material under constant load and constant temperature in the primary creep region is assumed (ref. 6) to be

$$\epsilon = \frac{\sigma}{E} + At^k \sinh \frac{\sigma}{\sigma_o} \tag{1}$$

where the creep strain is

$$\left(\epsilon - \frac{\sigma}{E}\right) = At^k \sinh \frac{\sigma}{\sigma_o} \tag{1a}$$

The term representing elastic strain, σ/E, must be modified to include plasticity if σ is above the elastic limit of the material. Since the creep strain at rupture is approximately constant regardless of stress and time, it may be assumed that the creep strain at rupture may be described by an equation similar to equation (1a). Creep rupture time under constant load is therefore taken to be given by the relation

$$t_r = \frac{C}{\sinh^{1/k} \frac{\sigma}{\sigma_o}} \tag{2}$$

Equations (1) and (2) are used in the formulation of relations describing creep behavior under varied loads.

Creep Relations for Varied Loads and Constant Temperature

The hypotheses studied during this investigation for the prediction of creep strain were the time-hardening, strain-hardening, and life-fraction rules. A brief description of these hypotheses is presented in the following sections and an analytical formulation of each is included for prediction of creep strain.

Time-hardening hypothesis.- In accordance with the time-hardening hypothesis, the creep behavior of a material at any stress level depends upon the stress and the total time which has elapsed since the instant of load application. The application of this rule is illustrated in figure 1(a). A material is subjected to an initial stress σ_A which produces creep strain ϵ_A at time t_A (point A in fig. 1(a)); the stress is then increased to σ_B. The time spent during the load change is assumed to be negligible in comparison with the time spent at each load level. The material will continue to creep under stress σ_B and will follow the σ_B curve beginning at point B, as indicated by the arrow, where $t_B = t_A$. Similarly, when the stress is changed again, the subsequent creep rate is determined by the time at which the stress change occurs and by the new stress level. The expression for accumulated strain predicted by the time-hardening hypothesis is

$$\epsilon_i = \frac{\sigma_i}{E} + A \sum_{n=1}^{n=i} \left(t_n^k - t_{n-1}^k \right) \sinh \frac{\sigma_n}{\sigma_o} \tag{3}$$

in which each stress σ_n is applied for time $t_n - t_{n-1} = \Delta t_n$ and $t_0 = 0$. Equation (3) is derived in appendix A.

Strain-hardening hypothesis.- In accordance with the strain-hardening hypothesis, after the applied stress has been increased or decreased in a material subjected to varied-load creep conditions, the creep of the material is determined by the amount of creep strain which

has accumulated since the initial application of load. Thus in figure 1(b), when the stress is changed at point A, creep will continue as indicated by the arrow beginning at point B, which is the point on the curve where the creep strain $\epsilon_B = \epsilon_A$. As derived in appendix B the equation for strain according to the strain-hardening hypothesis is

$$\epsilon_i = \frac{\sigma_i}{E} + A\left(\sum_{n=1}^{n=i} \Delta t_n \sinh^{1/k} \frac{\sigma_n}{\sigma_o}\right)^k \tag{4}$$

Life-fraction hypothesis.- The life-fraction hypothesis generally yields results which fall between the results obtained by the rules already described, and is analogous to the cumulative damage concept used in fatigue. In accordance with this hypothesis, the creep behavior of a material is dependent on the fraction of rupture time which has been consumed. Thus when the stress is changed at point A (fig. 1(c)), creep will continue as indicated by the arrow starting at point B, where t_B is determined from the relation

$$\frac{t_B}{t_{rB}} = \frac{t_A}{t_{rA}} \tag{5}$$

In equation (5), t_{rA} and t_{rB} are the rupture times corresponding to σ_A and σ_B, respectively. The total strain under varied-load creep is given by

$$\epsilon_i = \frac{\sigma_i}{E} + A\left\{t_1^k \sinh \frac{\sigma_1}{\sigma_o} + \sum_{m=2}^{m=i} t_{rm}^k \left[\left(\sum_{n=1}^{n=i} \frac{\Delta t_n}{t_{rn}}\right)^k - \left(\sum_{n=1}^{n=i-1} \frac{\Delta t_n}{t_{rn}}\right)^k\right] \sinh \frac{\sigma_m}{\sigma_o}\right\} \tag{6}$$

Equation (6) is derived in appendix C. It is also shown in appendix C that for the case in which both equations (1) and (2) apply, equation (6) becomes mathematically equal to equation (4) which expresses the strain in accordance with the strain-hardening hypothesis.

Equivalent stress.- Material creep behavior under cyclic loads can be computed from the relations given for creep under constant load by use of an equivalent stress. The equivalent stress is defined as that stress which, when applied continuously, will produce rupture in the same time as was obtained under the varied stress condition. Thus

introduction of the equivalent stress concept reduces the cyclic-load case to an equivalent constant-load case, and an approximation of the strain and rupture can be conveniently determined from the equivalent case.

In appendix D the life-fraction hypothesis is used in conjunction with the creep rupture relation (eq. (2)) to derive expressions for the equivalent stress σ_e. A convenient expression for σ_e in cyclic-load creep is

$$\sinh \frac{\sigma_e}{\sigma_o} = \left(\frac{\sum_{n=1}^{n=j} \Delta t_n \sinh^{1/k} \frac{\sigma_n}{\sigma_o}}{\sum_{n=1}^{n=j} \Delta t_n} \right)^k \qquad (7)$$

where j is the number of load levels per cycle. Note that in order to evaluate σ_e from equation (7), only the first load cycle need be considered. Equation (7) is applicable for cases in which the longest time spent at any load level during one cycle is small in comparison with the total test time. Values of equivalent stress σ_e calculated from equation (7) may be substituted for σ in equations (1) and (2) in order to estimate strain and rupture, respectively, under cyclic-load creep.

TEST PROGRAM

Stress-strain and creep tests were conducted on tensile specimens of 2024-T3 aluminum-alloy sheet of 0.125-inch thickness at a temperature of 400° F. Stress-strain tests and constant-load creep tests were performed in order to determine the empirical constants in equations (1) and (2). The stress-strain tests were performed at exposure times ranging from 0.5 hour to 50 hours (table I); and constant-load creep tests were conducted over a stress range from 10 ksi to 55 ksi (table II).

Nominal stresses applied during the varied-load creep tests ranged from 30 ksi to 45 ksi $\left(\text{approximately } \frac{2}{3}\ \sigma_{ty} \text{ to } \sigma_{ty}\right)$. The various types of load histories applied during the varied-load creep tests are illustrated in figure 2. Two-load tests represented in figure 2(a) consisted of two load applications, the second load level being applied until

rupture occurred. Cyclic-load creep tests consisted of repeated load cycles comprising two or three load levels each. Some load-time conditions were applied so that the durations of application of all load levels were equal. Other load cycles were such that the ratio of load duration to the corresponding constant-load rupture time was approximately the same for all loads.

The conditions for the varied-load creep tests are given in table III. The majority of these tests were conducted with the loads in ascending sequence within each cycle, as shown in figure 2. However, for each load history investigated, at least one test was performed with the load levels in descending sequence. This procedure afforded a direct indication of the influence of sequence of load application on the varied-load creep behavior of the material. Other details concerning the test specimens, equipment, and procedures may be found in appendix E.

RESULTS AND DISCUSSION

In this section, calculated and experimental results for creep under cyclic loading and constant temperature are presented and compared. Stress-strain and constant-load creep data which were used for evaluating constants necessary for computing cyclic-load creep behavior are also included.

Creep Under Constant Load

Results of stress-strain tests are given in table I and figure 3, and demonstrate the variation with exposure time characteristic of 2024-T3 aluminum-alloy sheet at 400° F. Creep data under constant load were obtained over a stress range from 10 ksi to 55 ksi. The 55-ksi stress is above the tensile yield stress of the material, as indicated by the stress-strain results. Results of the constant-load creep tests are tabulated in table II, and the creep curves are shown in figure 4. Tests performed at stresses below 30 ksi were discontinued when a significant amount of creep had occurred. No strain record was obtained during the creep test conducted at 55 ksi.

The empirical constants appearing in equations (1) and (2) were evaluated from the stress-strain and constant-load creep data. Determination of the creep constants was made on the basis of the creep data obtained at all stress levels. The values obtained are as follows:

$$E = 9.4 \times 10^3 \text{ ksi}$$

$$A = 6.8 \times 10^{-5}$$

$$k = 0.5$$

$$\sigma_o = 9.3$$

$$C = 1.25 \times 10^4$$

Constant-load creep curves computed from equation (1a), with the use of these values of the constants, are compared with the average experimental results in figure 5 to indicate the fit between the experimental data and the calculated curves. The constant-load creep-rupture curve calculated from equation (2) is shown in figure 6 together with experimental results.

Creep Under Varied Loads

The load histories which were applied during varied-load creep tests and the corresponding equivalent stresses are given in table III, together with experimental rupture times. Creep curves under varied loads are shown in figures 7 to 10. Calculated results are represented by solid lines. Experimental data are denoted by symbols, and dashed lines have been drawn through the data to show the trends more clearly. In each case the corresponding load history is shown in the figure.

Two-load creep.- The results of creep tests during which two loads were applied until rupture occurred are shown in figure 7. In each test the load was changed at approximately one-half the rupture time corresponding to the initial load. Under the initial load the experimental creep curves follow the calculated constant-load curves which are shown in the figure as solid lines. The effect of the load change on creep rate is clearly evident in the figure. Load increase resulted in a marked increase in creep rate, and rupture was imminent. On the other hand a decrease in applied load severely retarded the creep process, and rupture occurred well beyond the rupture time of the lower load. The duration of the first load during these tests produced creep strains that were generally beyond the primary creep stage. Equations (3), (4), and (6) were developed to describe cyclic-load creep behavior in the primary stage, and therefore are not applicable to the two-load tests performed.

Cyclic-load creep.- Creep strains computed for cyclic load from the time-hardening rule (eq. (3)) and the strain-hardening rule (eq. (4))

are compared in figure 8. Results predicted by the life-fraction rule are identical with calculations made by the strain-hardening hypothesis in this study because of the rupture expression used. The creep strains obtained from the time-hardening hypothesis yield lower strain rates and a smoother curve than the results obtained from the strain-hardening hypothesis. The strain-hardening hypothesis predicts higher creep strain than the time-hardening hypothesis when the load cycle is in ascending sequence and lower creep strain when the load cycle is in descending sequence. The curve for the equivalent stress approximation coincides at the end point of each cycle with the results from the life-fraction rule; this is a result of the assumptions on which the derivation of the equivalent stress is based (see appendix D). The hypotheses investigated can be expected to compare with one another in the same general fashion under other load histories.

Calculated creep strain is compared with experimental creep strain in figures 9 and 10. Figure 9 shows results involving two load levels per cycle; figure 10 represents creep results in which three load levels were applied per cycle. In each case the calculated results cover the range of creep strain generally considered to be of most interest in aircraft structural applications; that is, up to approximately 0.005. For each test the constant-load creep curves computed from equation (1a) for the stresses involved are also shown in the figures for comparison.

The hypotheses investigated yield results that are in fair agreement with experimental data at low creep strain when the load cycle is in ascending sequence, although the agreement is not as good when the load cycle is in descending sequence. None of the hypotheses is consistently superior to the others. Calculated strain values are in all cases somewhat higher than the strains obtained during the tests, particularly when the high load is applied first, up to approximately 0.004. These results appear to be due in part to the fact that the creep hypotheses do not take into account the effects of creep recovery when load is decreased. Beyond a creep strain of 0.004, the increasing slope of the experimental data signifies that the tests are beyond the primary creep stage and therefore the creep equations formulated no longer are applicable. The equivalent stress approach gives creep results which coincide at the end of each cycle with the strain-hardening results shown and are parallel to the constant-load creep curves.

Rupture.- Experimental rupture times obtained in varied-load creep tests are presented in table III and are plotted against calculated equivalent stress in figure 11. The solid line in the figure represents rupture times computed from equation (2) with σ_e substituted for σ. Reversing the sequence of load application appears to have no effect on the rupture time of cyclic tests. Agreement with experimental values is satisfactory, except for the two-load tests in which the higher load

was applied first. As already mentioned the two-load tests terminated much later than would be predicted for constant-load rupture tests.

CONCLUDING REMARKS

The time-hardening, strain-hardening, and life-fraction hypotheses have been formulated in mathematical terms in order to calculate creep behavior under varied load conditions based on a knowledge of material creep behavior obtained under constant load. A limited comparison of these theories has been carried out with the use of tensile creep data obtained from 2024-T3 aluminum-alloy sheet material at 400° F under cyclic-load conditions. Results show that all the hypotheses investigated predict similar creep strain results in the region of low strain. However the hypotheses generally yield somewhat higher strain values than those obtained experimentally, since the formulas derived do not include the retarding effects of creep recovery when the load is reduced during a test.

An equivalent stress has been defined for varied-load tests based on the life-fraction rule; this stress can be substituted directly into the material creep laws in order to estimate creep strain and rupture under cyclic loads. Rupture times computed for cyclic-load tests by making use of the equivalent stress are in satisfactory agreement with test results. Experimental rupture time appears to be independent of loading sequence, except in the two-load tests. Considerably different rupture times were obtained in the two-load tests depending on the order of application of load.

Although considerable study is necessary in order to explain the recovery phenomenon as it affects cyclic-load creep and to modify the creep relations accordingly, it appears that when many load cycles are applied, as in aircraft structural applications, the existing hypotheses produce fair agreement between calculated and experimental creep strain if the loads within the cycles are in ascending order. Poorer correlation is obtained when the loads within the cycles are in descending order. Rupture times computed using the life-fraction hypothesis were found to be in good agreement with experimental data.

Langley Research Center,
National Aeronautics and Space Administration,
Langley Field, Va., February 3, 1961.

APPENDIX A

APPLICATION OF TIME-HARDENING HYPOTHESIS TO VARIED-LOAD CREEP

In accordance with the time-hardening rule, the creep behavior of a material at any stress is determined by the total time elapsed. (See fig. 1(a).) Assume that a varied-load creep test begins at stress σ_1 and time $t_0 = 0$ and continues until time t_1. (See fig. 2.) At t_1 the strain is expressed by equation (1) as

$$\epsilon_1 = \frac{\sigma_1}{E} + A t_1^k \sinh \frac{\sigma_1}{\sigma_o} \tag{A1}$$

The stress is changed to σ_2 and the test continues at the new stress level until t_2. At this time the strain is

$$\epsilon_2 = \frac{\sigma_2}{E} + A\left[t_1^k \sinh \frac{\sigma_1}{\sigma_o} + \left(t_2^k - t_1^k\right)\sinh \frac{\sigma_2}{\sigma_o}\right] \tag{A2}$$

Similarly at any stress σ_i and time t_i the total accumulated strain is given by the time-hardening hypothesis as follows:

$$\epsilon_i = \frac{\sigma_i}{E} + A\left[t_1^k \sinh \frac{\sigma_1}{\sigma_o} + \left(t_2^k - t_1^k\right)\sinh \frac{\sigma_2}{\sigma_o} + \ldots + \left(t_i^k - t_{i-1}^k\right)\sinh \frac{\sigma_i}{\sigma_o}\right] \tag{A3}$$

which becomes

$$\epsilon_i = \frac{\sigma_i}{E} + A \sum_{n=1}^{n=i} \left(t_n^k - t_{n-1}^k\right)\sinh \frac{\sigma_n}{\sigma_o} \tag{A4}$$

Equation (A4) was used to calculate the creep curves labeled "time-hardening" in figures 9 and 10.

APPENDIX B

APPLICATION OF STRAIN-HARDENING HYPOTHESIS TO VARIED-LOAD CREEP

In accordance with the strain-hardening rule, when the applied stress is changed during a creep test the ensuing creep is determined by the amount of creep strain which has already been achieved. (See fig. 1(b).) This hypothesis is expressed mathematically in this appendix.

Assume that a creep test commences at stress σ_1 and continues until time t_1; then the total strain is expressed by equation (1) as

$$\epsilon_1 = \frac{\sigma_1}{E} + A t_1^k \sinh \frac{\sigma_1}{\sigma_o} \tag{B1}$$

If the test continues at σ_2 until t_2, the strain is given by

$$\epsilon_2 = \frac{\sigma_2}{E} + A t_1^k \sinh \frac{\sigma_1}{\sigma_o} + A\left[t_1\left(\frac{\sinh \frac{\sigma_1}{\sigma_o}}{\sinh \frac{\sigma_2}{\sigma_o}}\right)^{1/k} + \Delta t_2\right]^k \sinh \frac{\sigma_2}{\sigma_1} - A t_1^k \sinh \frac{\sigma_1}{\sigma_o}$$

$$= \frac{\sigma_2}{E} + A\left(t_1 \sinh^{1/k} \frac{\sigma_1}{\sigma_o} + \Delta t_2 \sinh^{1/k} \frac{\sigma_2}{\sigma_o}\right)^k \tag{B2}$$

where $t_1\left(\frac{\sinh \frac{\sigma_1}{\sigma_o}}{\sinh \frac{\sigma_2}{\sigma_o}}\right)^{1/k}$ is the time necessary to achieve a creep strain equal to $\left(\epsilon_1 - \frac{\sigma_1}{E}\right)$ at stress σ_2, and where $\Delta t_2 = t_2 - t_1$. Similarly, at σ_3 and t_3,

$$\epsilon_3 = \frac{\sigma_3}{E} + A\left(\frac{t_1 \sinh^{1/k}\frac{\sigma_1}{\sigma_o} + \Delta t_2 \sinh^{1/k}\frac{\sigma_2}{\sigma_o}}{\sinh^{1/k}\frac{\sigma_3}{\sigma_o}} + \Delta t_3\right)^k \sinh\frac{\sigma_3}{\sigma_o}$$

$$= \frac{\sigma_3}{E} + A\left(t_1 \sinh^{1/k}\frac{\sigma_1}{\sigma_o} + \Delta t_2 \sinh^{1/k}\frac{\sigma_2}{\sigma_o} + \Delta t_3 \sinh^{1/k}\frac{\sigma_3}{\sigma_o}\right)^k \qquad (B3)$$

Thus at any stress σ_i and time t_i, strain predicted by the strain-hardening hypothesis is given by

$$\epsilon_i = \frac{\sigma_i}{E} + A\left(\sum_{n=1}^{n=i} \Delta t_n \sinh^{1/k}\frac{\sigma_n}{\sigma_o}\right)^k \qquad (B4)$$

Equation (B4) was used to compute the creep curves labeled "strain-hardening" in figures 9 and 10.

APPENDIX C

APPLICATION OF LIFE-FRACTION HYPOTHESIS TO VARIED-LOAD CREEP

The life-fraction rule was originally proposed as a cumulative-damage theory for use in fatigue problems (refs. 7 and 8), but also finds application in the varied-load creep problem. In the case of varied-load creep the hypothesis may be stated thus: In varied-load creep the creep strain is a function of the fraction of creep life which has been consumed. The mathematical formulation of the theory is presented here.

As in the previous appendixes, creep is initiated at stress σ_1 and continues until time t_1, when the strain is given by

$$\epsilon_1 = \frac{\sigma_1}{E} + At_1^k \sinh \frac{\sigma_1}{\sigma_o} \tag{C1}$$

After spending the duration Δt_2 at σ_2,

$$\epsilon_2 = \frac{\sigma_2}{E} + At_1^k \sinh \frac{\sigma_1}{\sigma_o} + A\left[\left(t_{r2}\frac{\Delta t_1}{t_{r1}} + \Delta t_2\right)^k - \left(t_{r2}\frac{\Delta t_1}{t_{r1}}\right)^k\right]\sinh \frac{\sigma_2}{\sigma_o} \tag{C2}$$

where t_{r1} and t_{r2} are the rupture times for σ_1 and σ_2, respectively. Then, at any stress σ_i and time t_i, the total strain as calculated by the life-fraction hypothesis is

$$\begin{aligned}\epsilon_i = \frac{\sigma_i}{E} &+ At_1^k \sinh \frac{\sigma_1}{\sigma_o} + A\left[\left(t_{r2}\frac{\Delta t_1}{t_{r1}} + \Delta t_2\right)^k - \left(t_{r2}\frac{\Delta t_1}{t_{r1}}\right)^k\right]\sinh \frac{\sigma_2}{\sigma_o} \\ &+ A\left[\left(t_{r3}\frac{\Delta t_1}{t_{r1}} + t_{r3}\frac{\Delta t_2}{t_{r2}} + \Delta t_3\right)^k - \left(t_{r3}\frac{\Delta t_1}{t_{r1}} + t_{r3}\frac{\Delta t_2}{t_{r2}}\right)^k\right]\sinh \frac{\sigma_3}{\sigma_o} \\ &+ \cdots + At_{ri}^k\left[\left(\sum_{n=1}^{n=i}\frac{\Delta t_n}{t_{rn}}\right)^k - \left(\sum_{n=1}^{n=i-1}\frac{\Delta t_n}{t_{rn}}\right)^k\right]\sinh \frac{\sigma_i}{\sigma_o} \\ &= \frac{\sigma_i}{E} + A\left\{t_1^k \sinh \frac{\sigma_1}{\sigma_o} + \sum_{m=2}^{m=i} t_{rm}^k\left[\left(\sum_{n=1}^{n=i}\frac{\Delta t_n}{t_{rn}}\right)^k - \left(\sum_{n=1}^{n=i-1}\frac{\Delta t_n}{t_{rn}}\right)^k\right]\sinh \frac{\sigma_m}{\sigma_o}\right\}\end{aligned} \tag{C3}$$

For the case when the rupture time is given by equation (2), it can be shown that the mathematical forms for the life-fraction and strain-hardening hypotheses are identical. After substitution for t_r from equation (2), equation (C3) becomes

$$\epsilon_i = \frac{\sigma_i}{E} + A\left\{ t_1^k \sinh \frac{\sigma_1}{\sigma_o} + \sum_{m=2}^{m=i} \left[\left(\sum_{n=2}^{n=i} \Delta t_n \sinh^{1/k} \frac{\sigma_n}{\sigma_o} \right)^k - \left(\sum_{n=1}^{n=i-1} \Delta t_n \sinh^{1/k} \frac{\sigma_n}{\sigma_o} \right)^k \right] \right\}$$

$$= \frac{\sigma_i}{E} + A\left[t_1^k \sinh \frac{\sigma_1}{\sigma_o} + \left(\sum_{n=1}^{n=i} \Delta t_n \sinh^{1/k} \frac{\sigma_n}{\sigma_o} \right)^k - t_1^k \sinh \frac{\sigma_1}{\sigma_o} \right]$$

$$= \frac{\sigma_i}{E} + A\left(\sum_{n=1}^{n=i} \Delta t_n \sinh^{1/k} \frac{\sigma_n}{\sigma_o} \right)^k \qquad (C4)$$

The fact that equation (C4) is identical to equation (B4) indicates that the strain-hardening and life-fraction rules are identical within the range of stress where both equation (1) for strain and equation (2) for rupture apply.

APPENDIX D

EQUIVALENT STRESS FOR VARIED-LOAD CREEP

In this appendix an equivalent stress for varied-load creep is derived from the life-fraction rule. The equivalent stress is defined as that stress which when applied continuously will produce rupture at the same time as the varied-stress condition. Thus any varied-load creep problem can be reduced to the equivalent constant-load problem by computation of the equivalent stress. The equivalent stress will be derived for the general case of a random distribution of load levels and for the case of cyclic-load creep in which a definite load cycle is repeated many times.

L 1 3 9 4

General Case

According to the life-fraction rule, creep failure occurs when the following relation is satisfied:

$$\sum_{n=1}^{n=i} \frac{\Delta t_n}{t_{rn}} = 1 \qquad \text{(D1)}$$

The rupture time at which equation (D1) is satisfied is given by

$$t_r = \sum_{n=1}^{n=i} \Delta t_n \qquad \text{(D2)}$$

However, in the general case of random loading, the time increment Δt_i is unknown. When this quantity is substituted from equation (D1) into equation (D2), the result is

$$t_r = \sum_{n=1}^{n=i-1} \Delta t_n \left(1 - \frac{t_{ri}}{t_{rn}}\right) + t_{ri} \qquad \text{(D3)}$$

Thus after substitution for t_{rn} and t_{ri} from equation (2) into equation (D3), and by use of the definition of the equivalent stress σ_e, the rupture time becomes

$$t_r = \sum_{n=1}^{n=i-1} \Delta t_n \left(1 - \frac{\sinh^{1/k} \frac{\sigma_n}{\sigma_o}}{\sinh^{1/k} \frac{\sigma_i}{\sigma_o}} \right) + \frac{C}{\sinh^{1/k} \frac{\sigma_i}{\sigma_o}} = \frac{C}{\sinh^{1/k} \frac{\sigma_e}{\sigma_o}} \qquad (D4)$$

Equation (D4) yields the expression for equivalent stress, namely

$$\sinh \frac{\sigma_e}{\sigma_o} = \sinh \frac{\sigma_i}{\sigma_o} \left[\frac{C}{C + \sum_{n=1}^{n=i-1} \Delta t_n \left(\sinh^{1/k} \frac{\sigma_i}{\sigma_o} - \sinh^{1/k} \frac{\sigma_n}{\sigma_o} \right)} \right]^k \qquad (D5)$$

Equation (D5) was used to calculate equivalent stress for the two-load tests reported in the text.

Special Case: Cyclic-Load Creep

When many repeated load cycles are applied during a test, an expression can be derived for the equivalent stress which is more convenient than equation (D5) by considering the load-time characteristics of one cycle. For the purpose of this derivation, it is assumed that rupture occurs at the end of a cycle. This assumption introduces negligible error in the calculated rupture time if failure occurs after many load cycles have been applied.

In view of the assumption, equations (D1) and (D2) may be written as

$$N \sum_{n=1}^{n=j} \frac{\Delta t_n}{t_{rn}} = 1 \qquad (D6)$$

and

$$t_r = N \sum_{n=1}^{n=j} \Delta t_n \tag{D7}$$

where N is the number of cycles to produce rupture and j is the number of load levels per cycle. The unknown N can be eliminated between equations (D6) and (D7); then with the use of equation (2) and the definition of equivalent stress, equation (D7) takes the form

$$t_r = C \sum_{n=1}^{n=j} \frac{1}{\Delta t_n \sinh^{1/k} \frac{\sigma_n}{\sigma_o}} \sum_{n=1}^{n=j} \Delta t_n = \frac{C}{\sinh^{1/k} \frac{\sigma_e}{\sigma_o}} \tag{D8}$$

which yields the relation for the equivalent stress as follows:

$$\sinh \frac{\sigma_e}{\sigma_o} = \left(\frac{\sum_{n=1}^{n=j} \Delta t_n \sinh^{1/k} \frac{\sigma_n}{\sigma_o}}{\sum_{n=1}^{n=j} \Delta t_n} \right)^k \tag{D9}$$

The equivalent stress for any varied-load creep test can be calculated from equation (D5) or equation (D9), and the creep strain and rupture time can then be estimated by substituting the computed σ_e into equations (1) and (2), respectively.

APPENDIX E

TEST SPECIMENS, EQUIPMENT, AND PROCEDURE

The test specimens used in this study were machined from a single sheet of 2024-T3 aluminum alloy of 0.125-inch thickness. The specimens were 1 inch wide, with a length of 24 inches oriented in the rolling direction of the sheet. The width of each specimen was reduced to 1/2 inch along a 2-inch gage length in the center section.

Two testing machines were used to conduct the tests reported in this paper. The first is a conventional deadweight beam-loading type of creep machine used to apply constant loads. It is equipped with automatic temperature controls and an autographic strain recorder. Most of the constant-load and two-load creep tests were performed in this machine. All other tests were conducted with the equipment shown in figure 12. The varied-load creep testing machine shown was used to apply constant load with the weight cage, and to apply varying loads with the load-programing equipment and the hydraulic cylinder.

The load programer consists of ten channels with which up to ten different load levels can be controlled. The specific load levels chosen can be cycled repeatedly in a prescribed order, and random cycling can also be programed. Prior to a test each channel to be used is set for the desired load level and time at load. An additional channel is available for performing stress-strain tests. In operation, the load programer transmits the preset signal to an electrohydraulic servovalve. The servovalve transforms the electric signal into a pressure difference across the piston in the loading cylinder, and thus load is applied to the specimen. A mechanical spring-dashpot system was installed in series with the loading cylinder to permit greater control of finite load changes.

The load programing system does not contain an automatic comparison component between the controller and the applied load. For this reason the equipment required periodic monitoring and tests were interrupted overnight. Results of several constant-load creep tests conducted in this machine showed that the overnight removal of load and cooling of the specimens produced negligible effects on the data obtained. Minor adjustments of the programer load settings were made occasionally during cyclic-load tests in order to maintain loads within ± 1 percent of the desired loads.

The automatically controlled furnaces used in the investigation maintained the test temperature along the gage length of the specimen within 5° F.

In both testing machines, the strain of the specimens was measured by averaging the output of two microformers which were attached to the specimen gage points by a strain transfer device. Strain-time curves were recorded autographically on previously calibrated recorders.

REFERENCES

1. Isaksson, Åke: Krypning vid Variabel Spänning och Temperatur Bibliografi. (Bibliography on Creep Under Variable Stress and Temperature.) Pub. Nr. 116, Div. of Strength of Materials, Roy. Inst. Tech. (Stockholm), 1957.

2. Manson, S. S., and Brown, W. F., Jr.: A Survey of the Effects of Nonsteady Load and Temperature Conditions on the Creep of Metals. Proc. Fourth Sagamore Ord. Materials Research Conf. - High Temperature Materials, Their Strength Potentials and Limitations (Contract DA-30-115-ORD-854), Syracuse Univ. Res. Inst., Aug. 1957, pp. 282-338.

3. Mathauser, Eldon E., Berkovits, Avraham, and Stein, Bland A.: Recent Research on the Creep of Airframe Components. NACA TN 4014, 1957.

4. Goldin, Robert: Thermal Creep Design Criteria. Aero. Eng. Rev., vol. 16, no. 12, Dec. 1957, pp. 36-41.

5. Mendelson, A., Hirschberg, M. H., and Manson, S. S.: A General Approach to the Practical Solution of Creep Problems. Paper No. 58—A-98, ASME, Nov.-Dec. 1958.

6. Deveikis, William D.: Investigation of the Compressive Strength and Creep of 7075-T6 Aluminum-Alloy Plates at Elevated Temperatures. NACA TN 4111, 1957.

7. Palmgren, Arvid: Die Lebensdauer von Kugellagern. (The Lifetime of Ball Bearings.) Z.V.D.I., Bd. 68, Nr. 14, Apr. 1924, pp. 339-341.

8. Miner, Milton A.: Cumulative Damage in Fatigue. Jour. Appl. Mech., vol. 12, no. 3, Sept. 1945, pp. A-159 - A-164.

TABLE I.- STRESS-STRAIN DATA

Test	Exposure time, hr	E, ksi	σ_{ty}, ksi
1	0.5	9.4×10^3	44.9
2	.5	9.4	44.7
3	2.0	9.4	51.3
4	5.0	9.4	45.8
5	20.0	9.4	42.6
6	20.0	9.4	42.3
7	50.0	9.4	38.9
8	50.0	9.4	38.8

TABLE II.- CONSTANT-LOAD RUPTURE DATA

Test	σ, ksi	Rupture time, hr
9	10	Test stopped at 90.0
10	10	Test stopped at 150.0
11	10	Test stopped at 46.0
12	15	Test stopped at 66.0
13	15	Test stopped at 55.0
14	20	Test stopped at 66.0
15	20	Test stopped at 45.0
16	25	Test stopped at 53.0
17	25	Test stopped at 45.0
18	25	Test stopped at 50.0
19	30	101.0
20	30	63.9
21	35	62.4
22	35	24.0
23	40	6.5
24	40	9.4
25	45	1.3
26	45	2.2
27	50	.9
28	50	1.8
29	50	.7
30	55	.2

TABLE III.- VARIED-LOAD CREEP TESTS

(a) Two-load tests

Test	σ_1, ksi	Δt_1, hr	σ_2, ksi	Δt_2	σ_e, ksi	Experimental rupture time, hr
31	40	4.0	45	To rupture	42.1	5.8
32	45	1.1	40	To rupture	41.3	18.0
33	45	1.1	40	To rupture	41.3	25.7
34	30	50.5	40	To rupture	31.5	50.6
35	40	4.0	30	To rupture	32.4	211.7
36	40	5.0	30	To rupture	33.3	527.5
37	40	6.5	30	To rupture	34.8	115.1

(b) Two-step cyclic tests

Test	σ_1, ksi	Δt_1, hr	σ_2, ksi	Δt_2, hr	σ_e, ksi	Experimental rupture time, hr
38	41.3	0.100	46.3	0.100	44.5	2.6
39	46.3	.100	41.3	.100	44.5	2.3
40	41.3	.157	46.3	.043	43.0	3.4
41	46.3	.043	41.3	.157	43.0	4.5
42	31.3	.200	41.3	.200	38.6	20.0
43	41.3	.200	31.3	.200	38.6	14.0
44	31.3	.927	41.3	.073	33.3	39.9
45	41.3	.073	31.3	.927	33.3	29.0

(c) Three-step cyclic tests

Test	σ_1, ksi	Δt_1, hr	σ_2, ksi	Δt_2, hr	σ_3, ksi	Δt_3, hr	σ_e, ksi	Experimental rupture time, hr
46	31.3	0.200	36.3	0.200	41.3	0.200	37.9	13.0
47	41.4	.200	36.4	.200	31.4	.200	38.0	14.4
48	31.3	.730	36.3	.212	41.3	.058	34.2	23.0
49	31.3	.730	36.3	.212	41.3	.058	34.2	24.0
50	41.3	.058	36.3	.212	31.3	.730	34.2	30.0

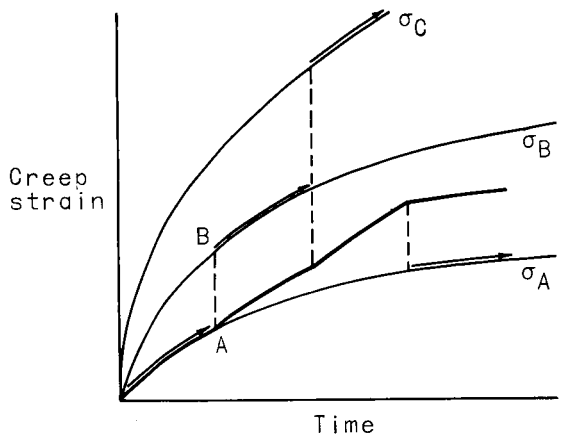

(a) Time-hardening hypothesis.

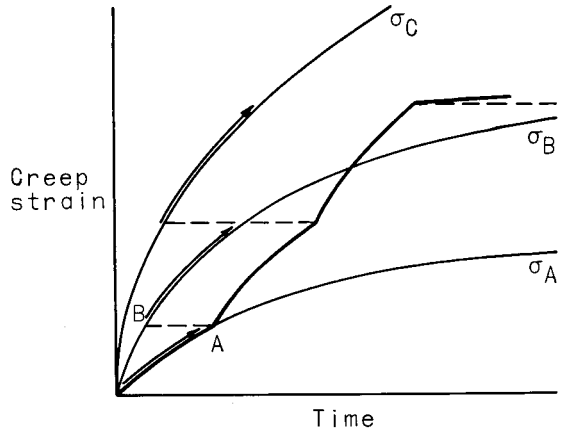

(b) Strain-hardening hypothesis.

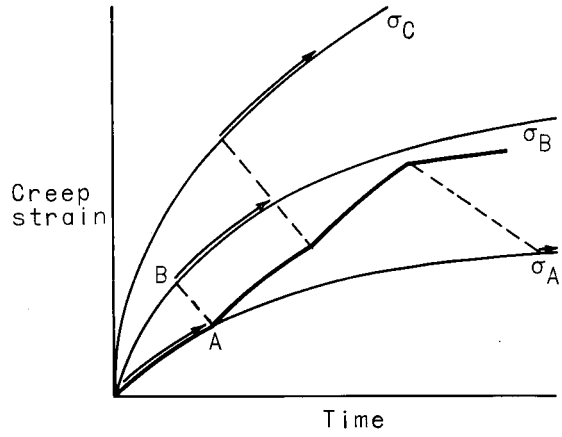

(c) Life-fraction hypothesis.

Figure 1.- Illustration of three hypotheses for varied-load creep.

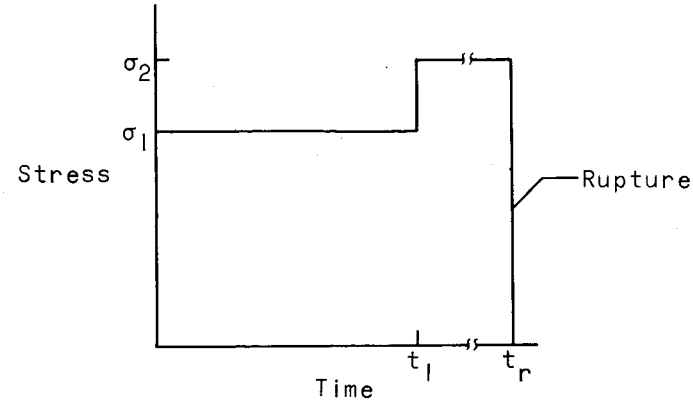

(a) Two-load test.

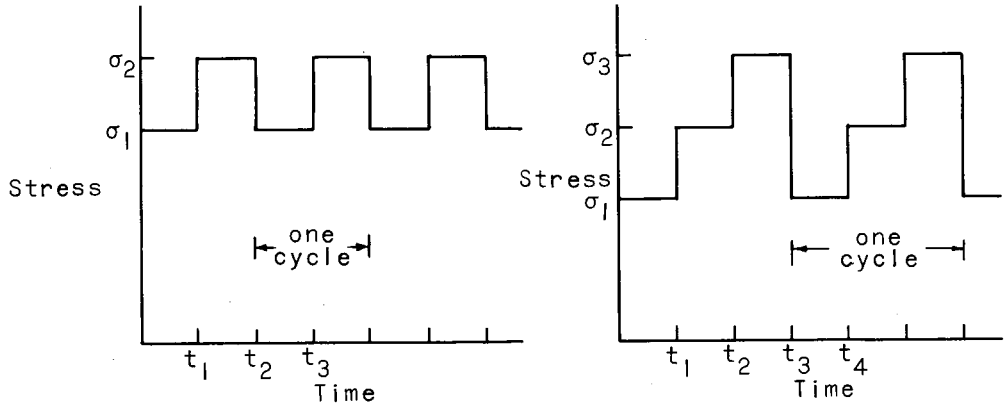

(b) Equal-time load steps.

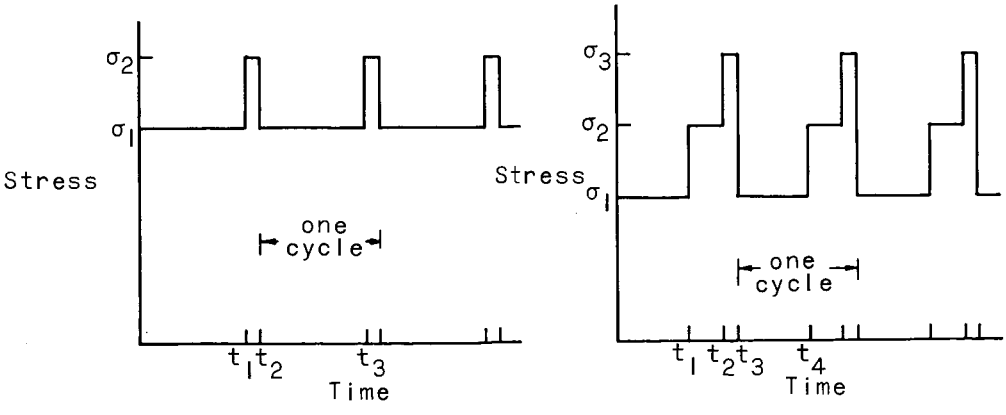

(c) Equal-life-fraction load steps.

Figure 2.- Types of load histories applied in tests.

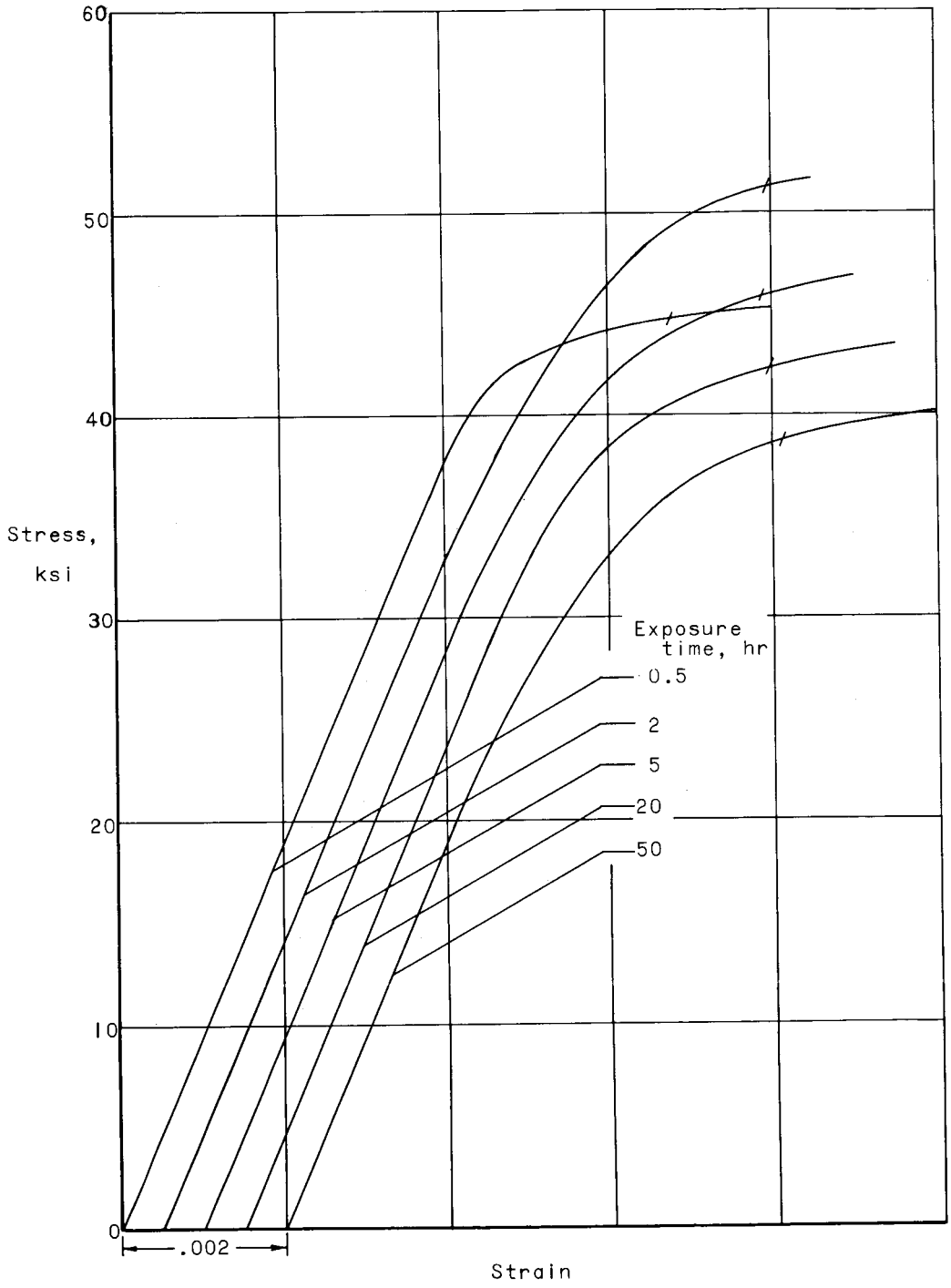

Figure 3.- Tensile stress-strain curves for 2024-T3 aluminum-alloy sheet at 400° F.

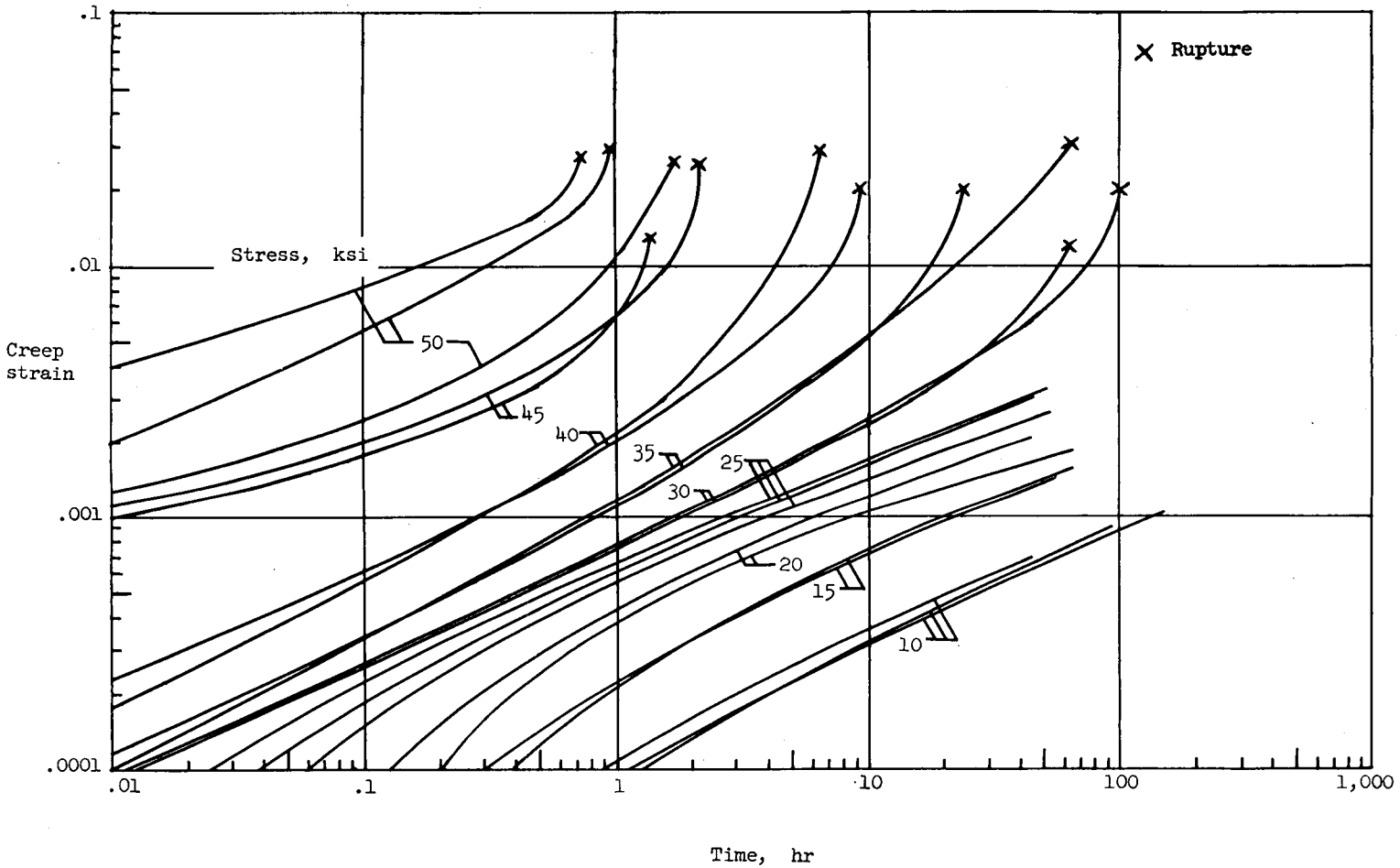

Figure 4.- Tensile creep curves for 2024-T3 aluminum-alloy sheet at 400° F. 0.5-hour exposure to test temperature prior to loading.

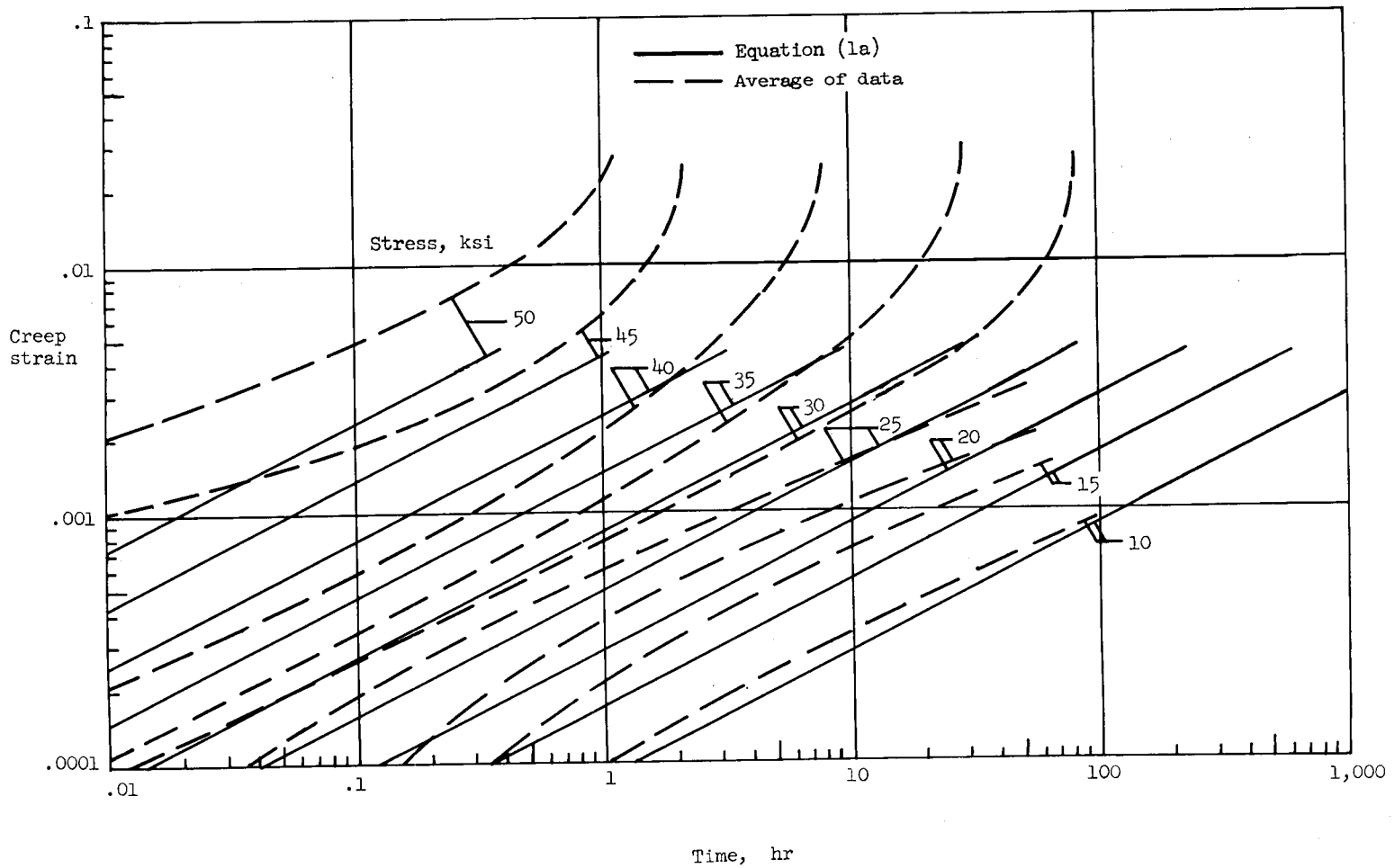

Figure 5.- Comparison of creep curves calculated from equation (1a) with experimental data obtained from 2024-T3 aluminum-alloy sheet at 400° F.

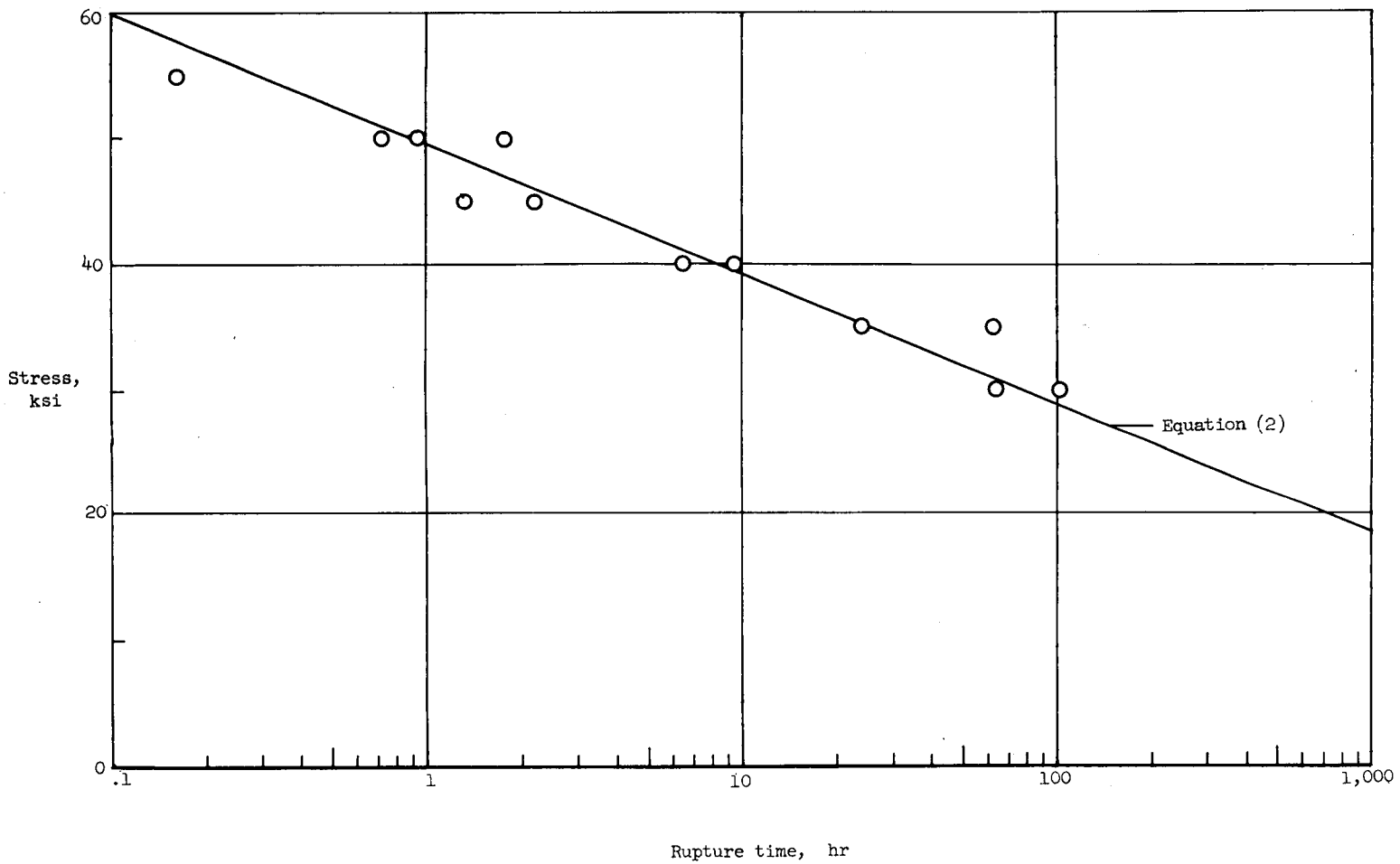

Figure 6.- Effect of stress on creep rupture time of 2024-T3 aluminum-alloy sheet under constant load at 400° F.

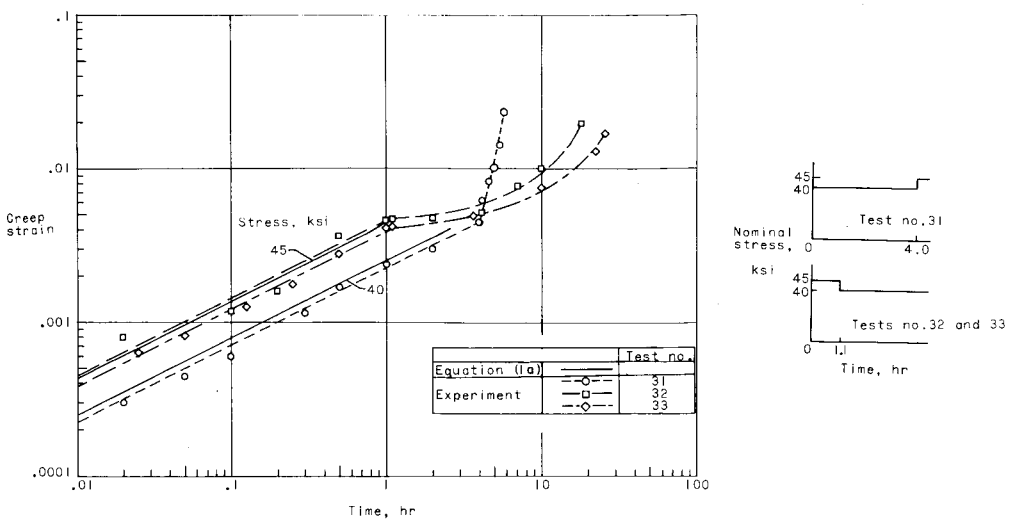

(a) Tests 31 to 33.

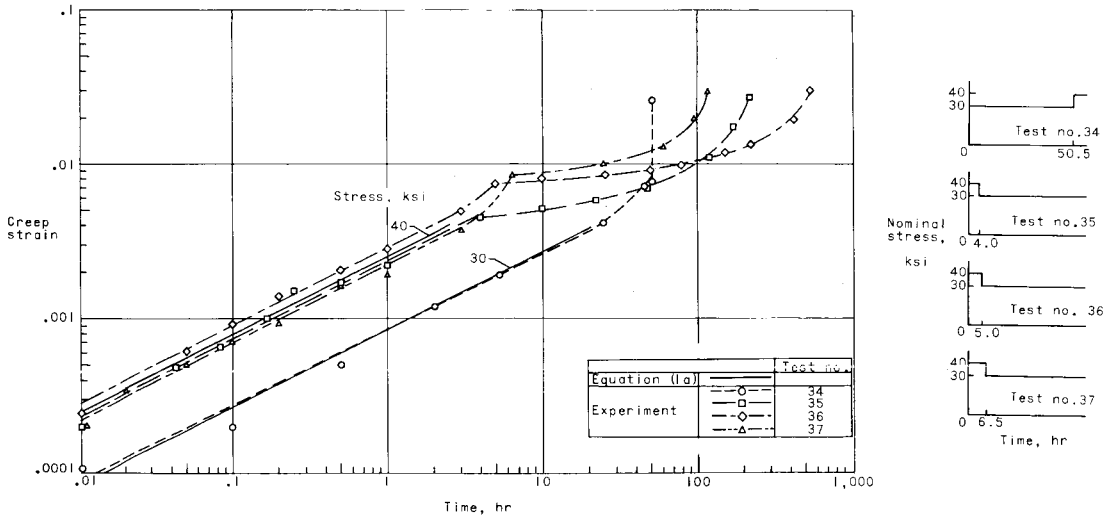

(b) Tests 34 to 37.

Figure 7.- Creep curves for two-load tests on 2024-T3 aluminum-alloy sheet at 400° F.

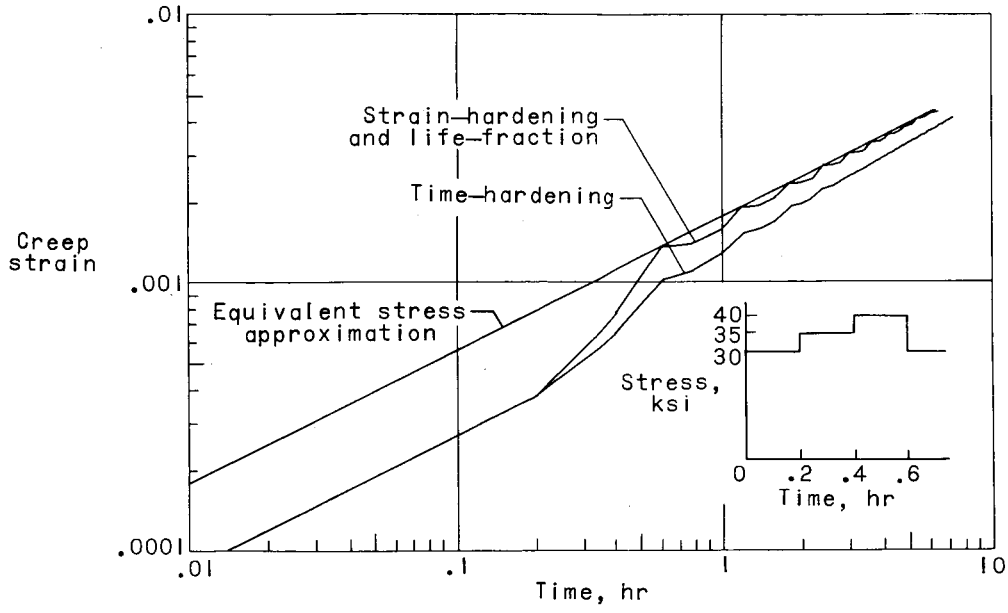

(a) Loads in ascending sequence.

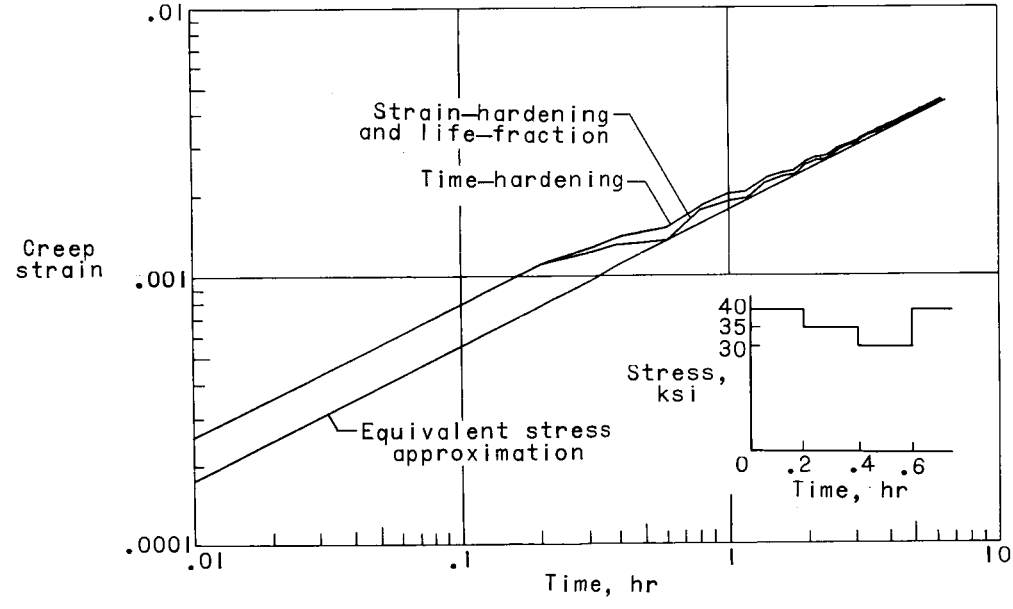

(b) Loads in descending sequence.

Figure 8.- Comparison of creep curves for cyclic-load creep calculated by the strain-hardening, time-hardening, and life-fraction hypotheses.

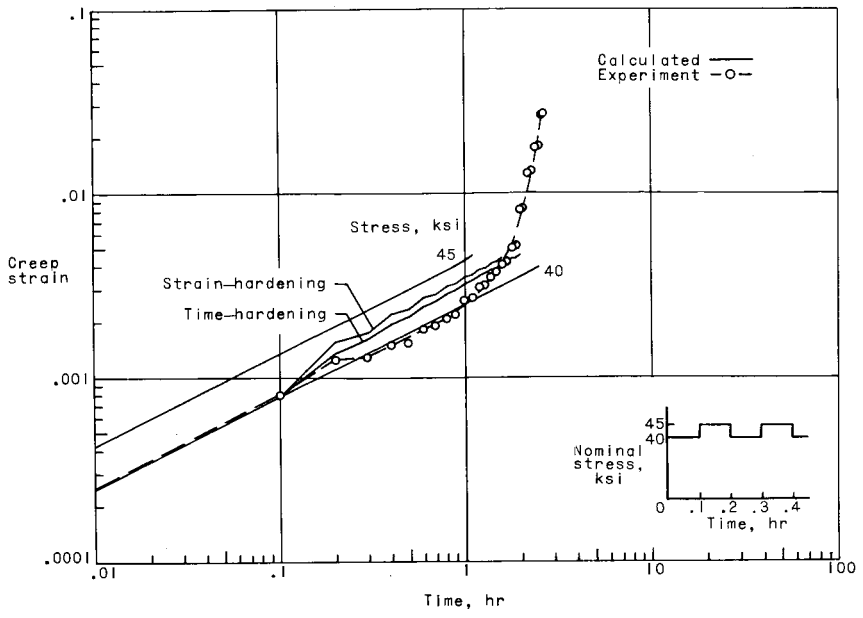

(a) Test 38.

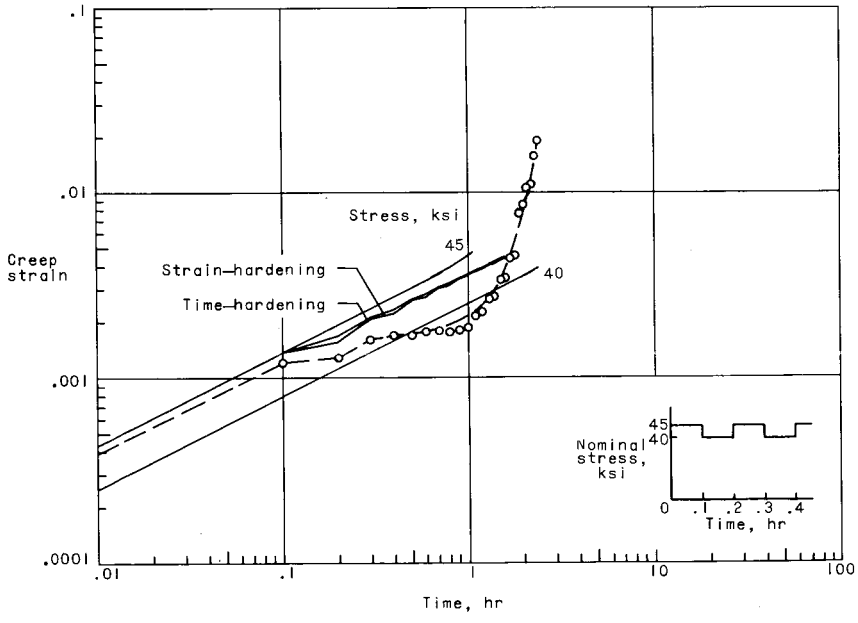

(b) Test 39.

Figure 9.- Two-step cyclic-load creep curves for 2024-T3 aluminum-alloy sheet at 400° F.

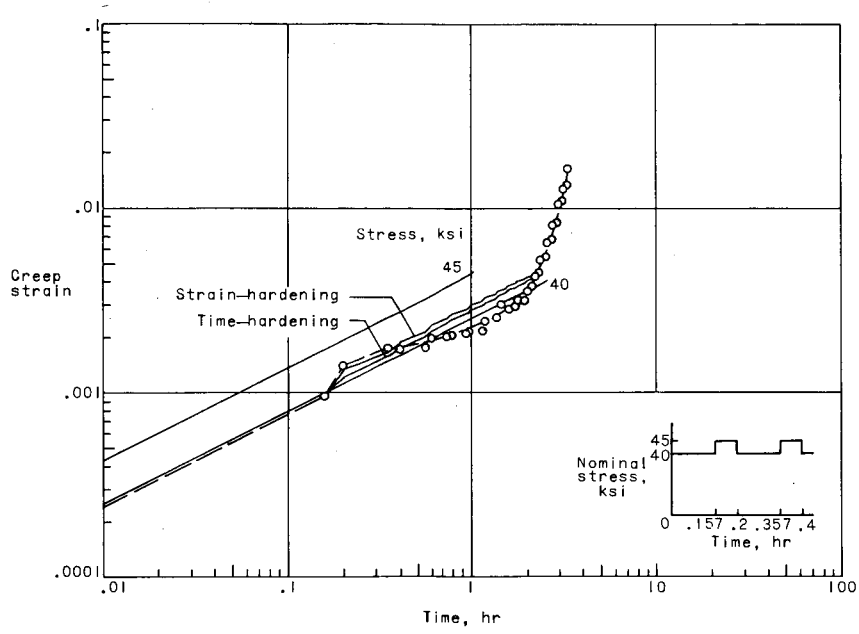

(c) Test 40.

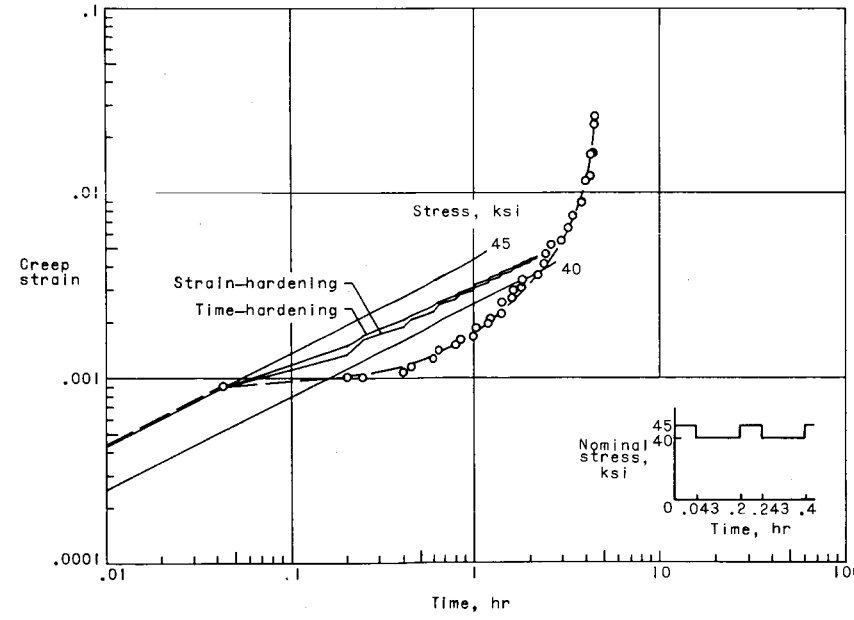

(d) Test 41.

Figure 9.- Continued.

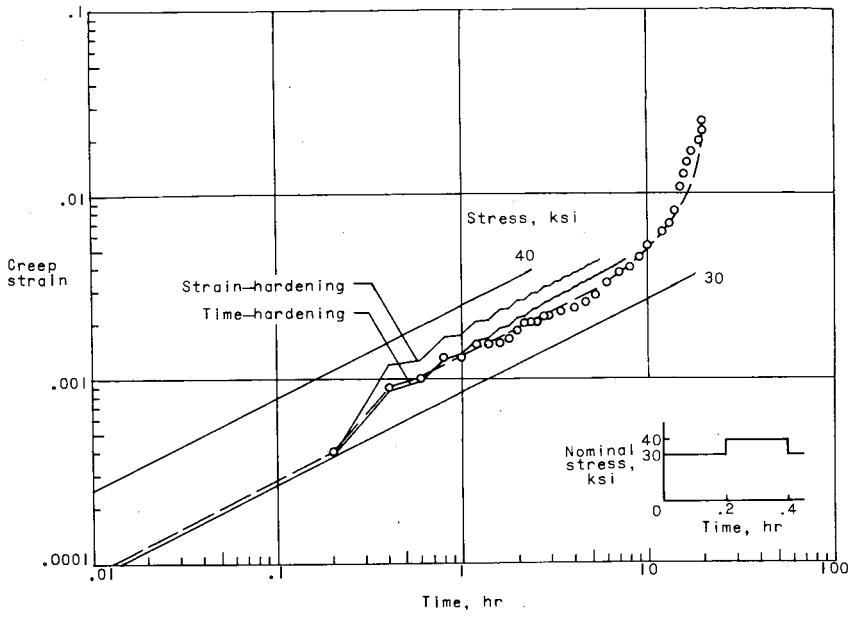

(e) Test 42.

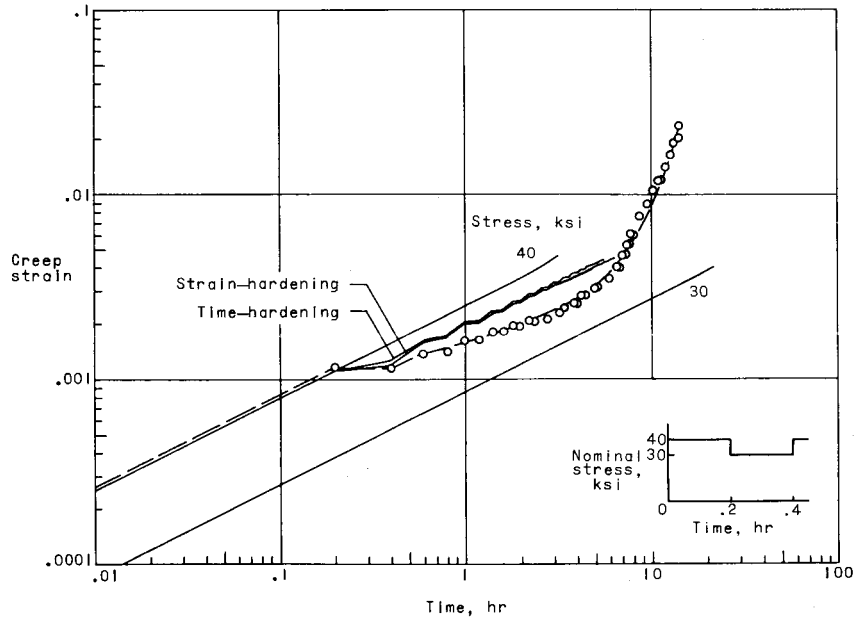

(f) Test 43.

Figure 9.- Continued.

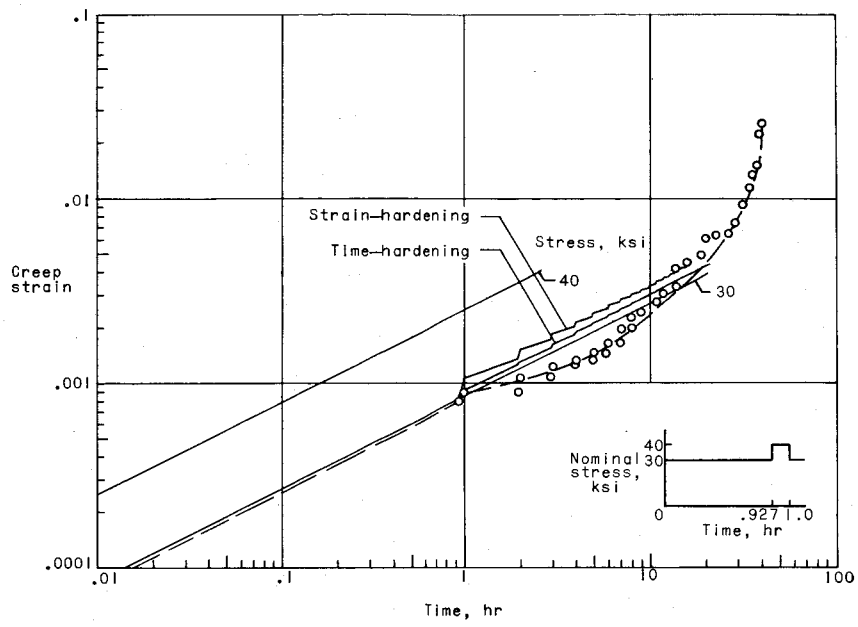

(g) Test 44.

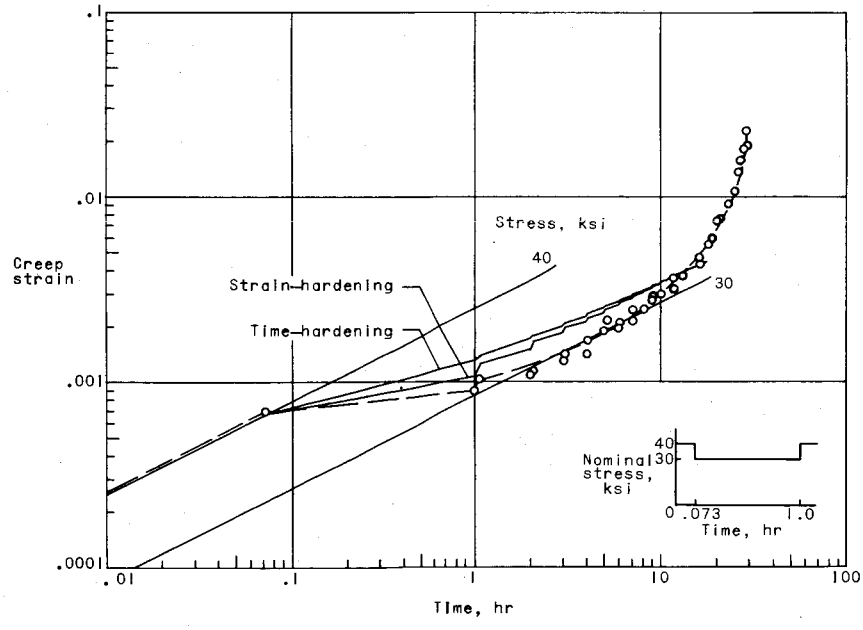

(h) Test 45.

Figure 9.- Concluded.

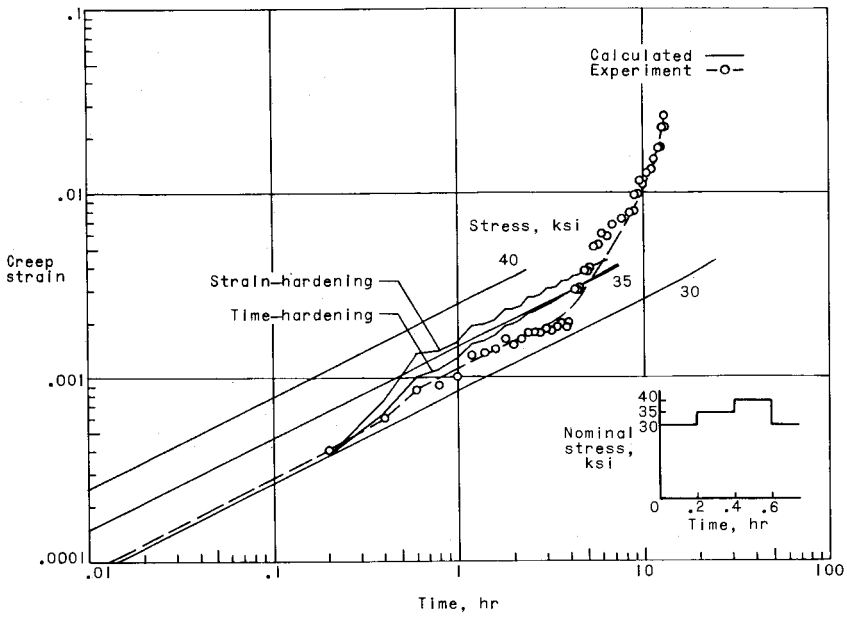

(a) Test 46.

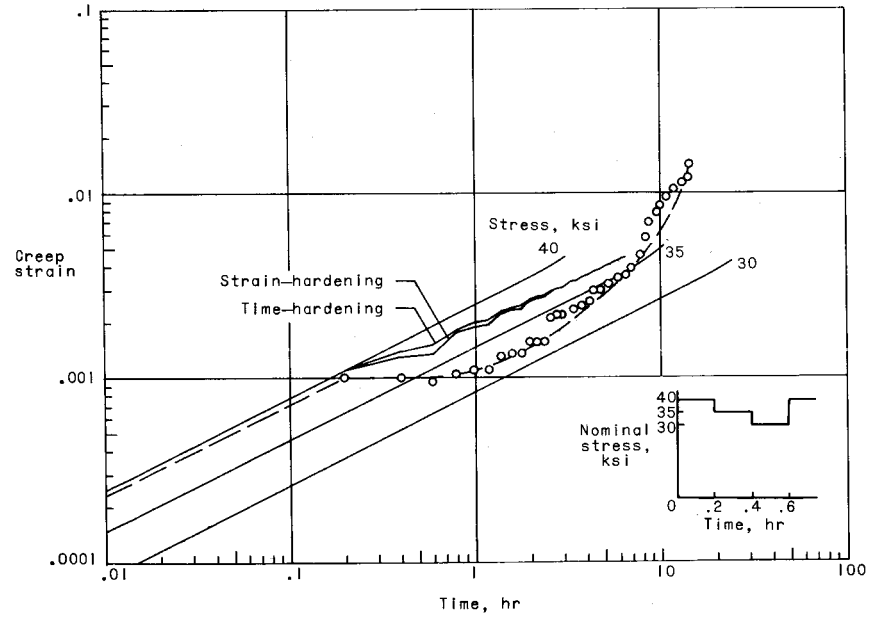

(b) Test 47.

Figure 10.- Three-step cyclic-load creep curves for 2024-T3 aluminum-alloy sheet at 400° F.

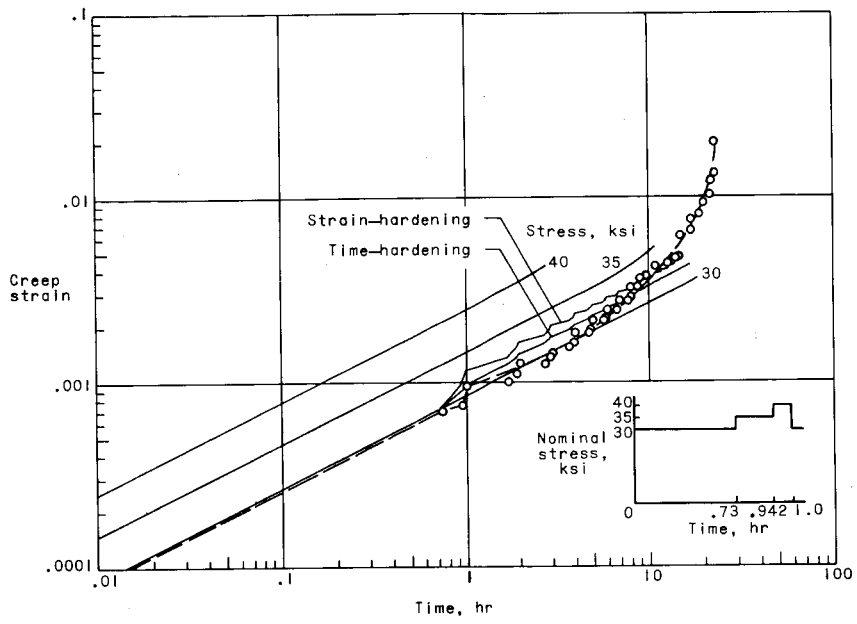

(c) Test 48.

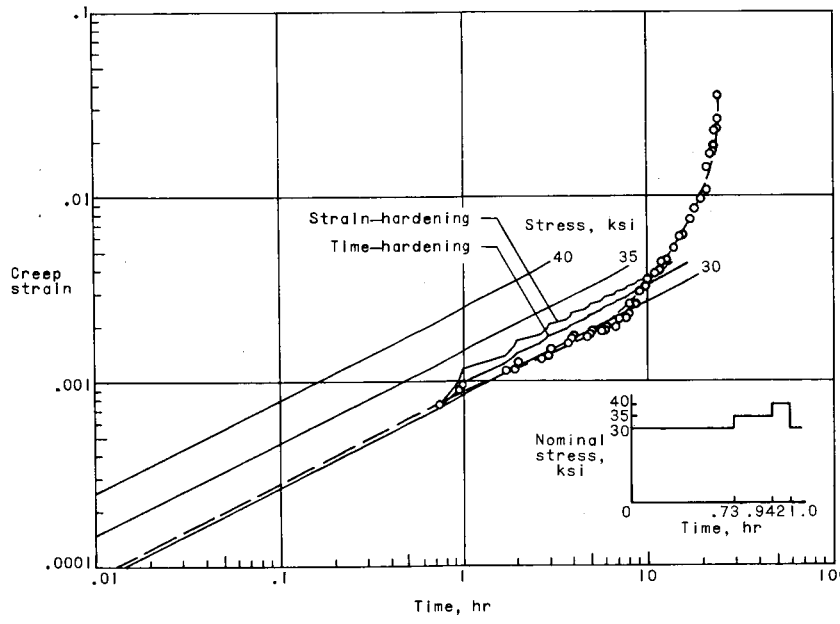

(d) Test 49.

Figure 10.- Continued.

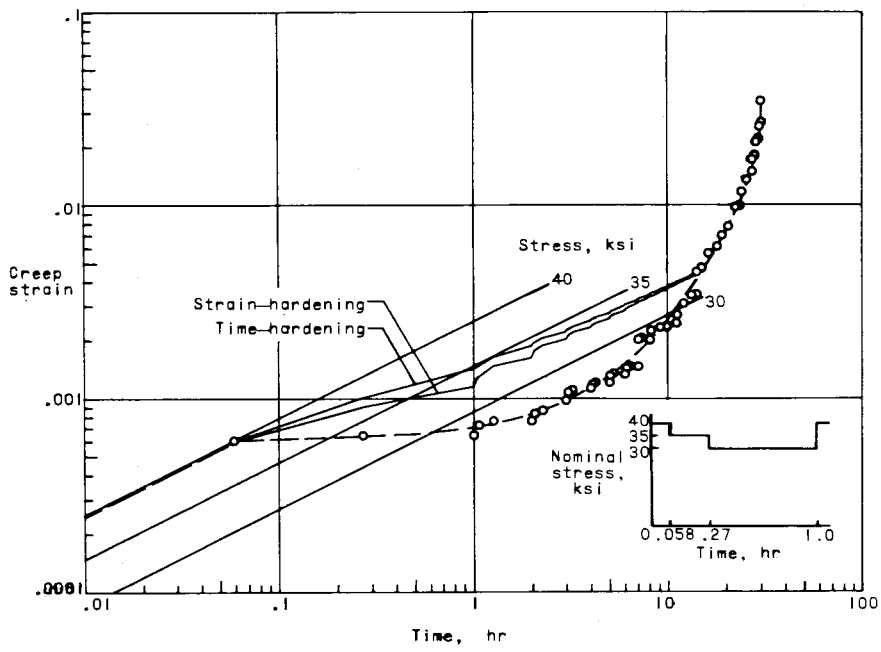

(e) Test 50.

Figure 10.- Concluded.

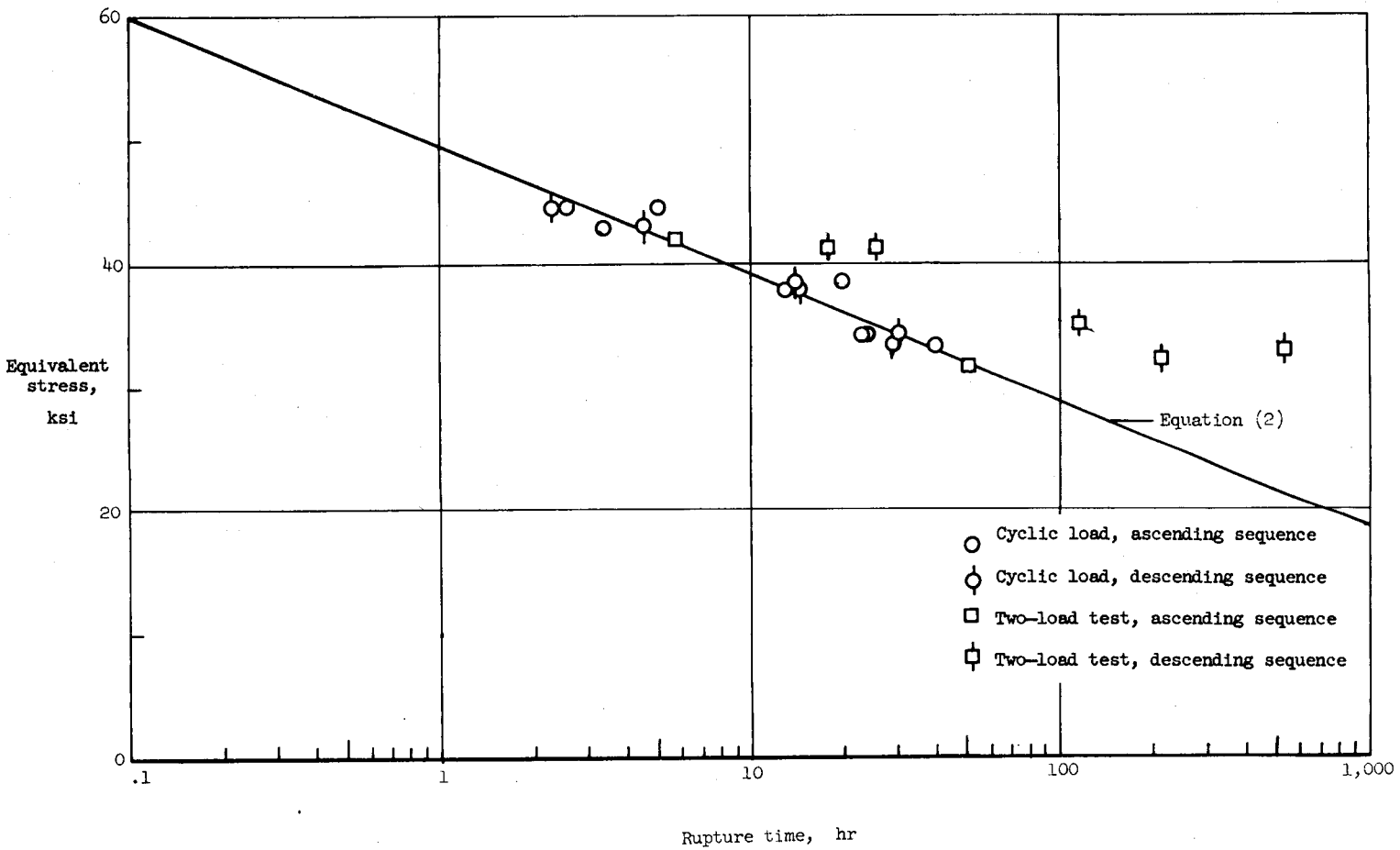

Figure 11.- Comparison of experimental and calculated rupture time of 2024-T3 aluminum-alloy sheet obtained in varied-load creep tests at 400° F.

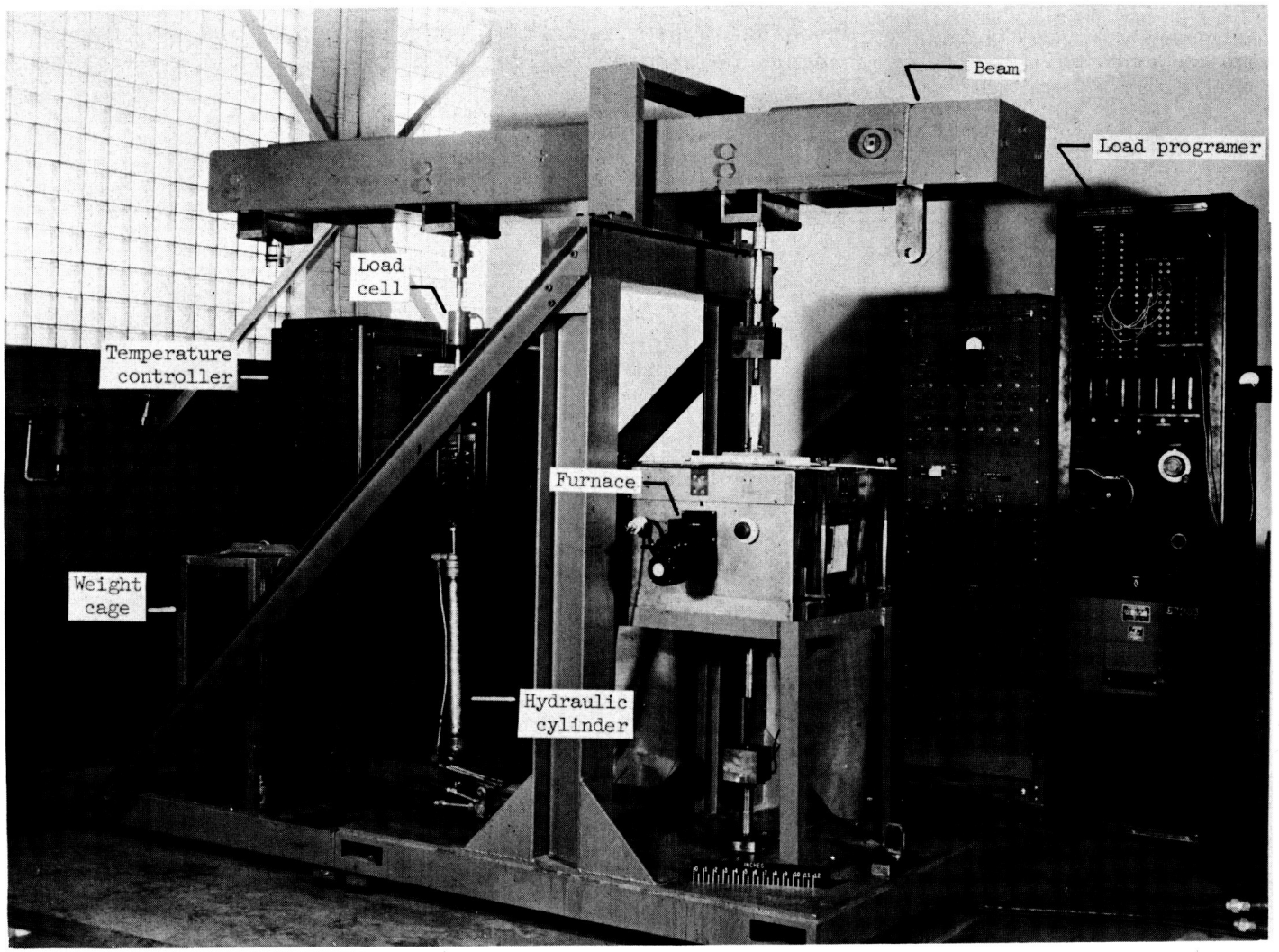

Figure 12.- Varied-load creep testing machine. L-59-7943.1